Experimental Bond Behaviour of GFRP and Masonry Bricks under Impulsive Loading

João M. Pereira [a]*, Paulo B. Lourenço [a]

[a] ISISE, Department of Civil Engineering, University of Minho, Guimarães, Portugal

* Corresponding author: Department of Civil Engineering, University of Minho, Campus de Azurém, Guimarães, 4800-058, Portugal; email: jpereira@civil.uminho.pt

Abstract: Fibre Reinforced Polymers have become a popular material for strengthening of masonry structures. The performance of this technique is strongly dependent on the bond between the FRP and the substrate. Understanding the strain rate effect on these materials and strengthening techniques is important for proper design and proper modelling of these systems under impacts or blast loads. This work aims to study the behaviour of the bond between GFRP and brick at different strain rates. A Drop Weight Impact Machine specially developed for pull-off tests (single shear tests) is used with different masses and different heights introducing different deformation rates. The strain rate effect on the failure mode, shear capacity and effective bond length is determined from the experimental results. Empirical relations of dynamic increase factors (DIF) for these materials and techniques are also presented.

Keywords: GFRP, Masonry, Impact, Drop Weight, Strain rate, DIF

1. Introduction

Different loading conditions might lead to different strain rates. Quasi-static loading produces strain rates of around 10^{-5} s^{-1}, while impacts and blast loading produce strain rates of well over 100 s^{-1}. When subjected to dynamic loading conditions, materials can have a much different behaviour when compared with their static behaviour (Meyers [1], Hiermaier [2], Ngo et al [3], Stavrogin and Tarasov [4]). Most research work on structural response and damage under impact and blast loading assumes typically static material properties (Baylot et al [5], Moreland et al [6].

In recent years, composites materials such as fibre reinforced polymers (FRPs) have been increasingly accepted as effective strengthening technique for civil engineering structures, particularly in the case of reinforced concrete and masonry (Bakis et al [7], Pampazopoulou et al [8]). The effectiveness of these strengthening techniques is strongly dependable on the bond behaviour between the substrate and the FRP fabric. Studies on the influence of the strain rates on the bond behaviour of these strengthening systems are scarce and cannot be found easily in the literature. Recently, Al-zubaidy et al [9] studied the bond behaviour between CFRP fabrics and steel plate joints under tensile loads with deformation rates up to 5 m/s. This work concluded that the use of multi-layer reinforcement was ineffective and the effective bond length was not affected by the deformation rate. They have also shown that the failure modes obtained under impulsive regime were similar to those obtained under quasi-static loading regime. Shi et al [10] studied the bond behaviour between FRP laminates and concrete using double-lap shear bond tests up to strain rates of 0.1 s^{-1}. These authors showed that for strain rates of 0.1 s^{-1} the increase in the ultimate shear strength is 1.3 times the quasi-static value. These authors also concluded that the influence of the strain rate is more pronounced for weaker concrete, and it is not significantly affected by the properties of

bonding adhesives and the type of FRP composite. Similar conclusions were obtained by other authors when studying the bond behaviour of different FRP laminates and concrete (Li et al [11], Shen et al [12]).

In order to fully understand the influence of the strain rates in these strengthening systems and to develop empirical relations able to estimate the response of these materials under high strain rates, it is necessary to study the substrate and the fabric independently and the strengthening systems itself.

Dynamic behaviour of common construction materials such as concrete (Grote et al [13]) or reinforcement bars (Malvar and Ross [14]) have been studied in recent years, being already introduced into some standards (CEB-FIP [15], UFC 3-340-02 [16]) in the form of a dynamic increase factor (DIF) which represents the ratio between the dynamic and static property. However, very limited studies can be found in the literature for masonry materials. Recently, Hao and Tarasov [17], Pereira et al [18], Lourenço and Pereira [19] and Asprone et al [20] studied this effect on masonry components (clay brick, stone and mortar) and masonry specimens. It was shown that Dynamic Increase Factors (DIF) up to 2.54 and 2.17, were obtained for the compressive strength of clay bricks and masonry at a strain rate of 200 s^{-1}. Similar values were obtained for the Young's modulus. Regarding the tensile behaviour of these materials, DIF up to 3.1 for the tensile strength of mortar joints were obtained at a strain rate of 1 s^{-1} and DIF up to 3 were obtained for the tensile strength of the tested stones. Composite materials were also studied under high strain rate effects in recent years and some of these studies (Gurusideswar and Velmurugan [21], Okoli [22] and Correira and Peixinho [23]) show that at strain rates of 500 s^{-1}, DIF up to 2 can be obtained for Glass Fibre Reinforced Polymer (GFRP) strips.

In this paper, an experimental campaign on the influence of the strain/deformation rate on the mechanical bond behaviour of GFRP-brick systems is described. The tests were performed with a Drop Weight tower developed specifically for this purpose. This equipment is able to perform single-lap shear bond tests under impulsive regime using a drop hammer being releases at a specific height. Both materials are studied independently previously – clay brick and GFRP strips – and in this paper the bond behaviour of the strengthening systems is studied under high deformation rates.

2. Clay brick under high strain rates

Studies on clay bricks under high strain rates were performed previously and were presented in detail by Pereira et al [18] and Lourenço and Pereira [19]. These bricks were of the same material used in the single-lap shear bond tests presented in the next section. A drop weight impact machine was used to perform the compression tests at different strain rates. Two different ways were used to measure the deformation profile: a) a FastCam video camera using targets in the specimen and video tracking software; b) strain gauges in all faces of the specimen Pereira et al [18], Lourenço and Pereira [19].

The results obtained by Pereira et al [18] and Lourenço and Pereira [19] can be seen in Figure 1. It is clear that these material show strain rate dependency. At a strain rate of 200 /s Dynamic Increase Factors of 2.54, 2.43, 1.30 and 5.95 were reported for the compressive strength, Young's modulus, strain at peak strength and compressive fracture energy, respectively. The obtained results are in agreement with other studies (Hao and Tarasov [17]). The empirical equations able to estimate these mechanical properties for strain rates up to 200 /s, as follows (Pereira et al [18], Lourenço and Pereira [19]):

For the compressive strength:

$$DIF(\sigma_u) = \begin{cases} 1 & if \quad 1E-5\ s^{-1} < \dot{\varepsilon} < 2\ s^{-1} \\ 0{,}3344 \ln(\dot{\varepsilon}) + 0.7682 & if \quad 2\ s^{-1} < \dot{\varepsilon} < 200\ s^{-1} \end{cases} \quad (1)$$

For the Young's modulus:

$$DIF(E) = \begin{cases} 1 & if \quad 1E-5\ s^{-1} < \dot{\varepsilon} < 2\ s^{-1} \\ 0{,}3105 \ln(\dot{\varepsilon}) + 0.7848 & if \quad 2\ s^{-1} < \dot{\varepsilon} < 200\ s^{-1} \end{cases} \quad (2)$$

For the strain at peak strength:

$$DIF(\varepsilon_u) = \begin{cases} 1 & if \quad 1E-5\ s^{-1} < \dot{\varepsilon} < 2\ s^{-1} \\ 0{,}0673 \ln(\dot{\varepsilon}) + 0.9533 & if \quad 2\ s^{-1} < \dot{\varepsilon} < 200\ s^{-1} \end{cases} \quad (3)$$

For the compressive fracture energy:

$$DIF(G_C) = \begin{cases} 1 & if \quad 1E-5\ s^{-1} < \dot{\varepsilon} < 5\ s^{-1} \\ 1{,}3419 \ln(\dot{\varepsilon}) - 1.1597 & if \quad 5\ s^{-1} < \dot{\varepsilon} < 200\ s^{-1} \end{cases} \quad (4)$$

3. GFRP under high strain rates

Correia and Peixinho [23] tested GFRP strips under different strain rates. The tested GFRP strips were of the same material used for the single-lap shear bond tests presented in the next section. Two different testing equipments were used allowing two different strain rate levels. A Servo-hydraulic testing machine (Instron, 25 kN capacity) was used for lower loading speed (0.02 mm/s), while a high-speed servo-hydraulic testing machine (Zwick, 20 kN capacity) was used for loading speed of approximately 6000 mm/s. Regarding the high-speed testing equipment, this includes a slack-response bracket, allowing the pull-rod to accelerate before commencing to load the specimen; the internal measuring systems of the equipment were used, including piezo-electric load cell and vertical displacement transducer for the stroke of the pull-rod. The

nominal strain rates obtained in the tests was calculated by dividing the linear speed of the testing machine by the parallel length of the specimen.

The results obtained by Correia and Peixinho [23] can be seen in Figure 2 and the strain rates varied from 0.655 /s to 446 /s. It is clear that this material shows strain rate dependency. The observed dispersion in the experimental results is somehow expected considering the impulsive nature of the experiments and the handmade building process of the specimens. In the higher strain rate tests a higher tensile strength was obtained, averaging 1862 MPa, while for the lower strain rate tests only a tensile strength of 1030 MPa (average) was obtained. This represents a Dynamic Increase Factor of about 1.8 for strain rates of about 500 /s. These results are in agreement with previous studies regarding similar materials and similar tests (Gurusideswar and Velmurugan [21], Okoli [22]).

4. Bond behaviour of GFRP-brick under high strain rates

In this work it is intended to study the effect of high strain rates in the bond behaviour of GFRP-brick strengthening systems. The main objective is to develop empirical relations, based on experimental results, able to relate the maximum bond capacity with the slip rate. These empirical relations are based on the DIF (Dynamic Increase Factor). During the tests both the load profile and slip profile are necessary. The load profile relates to the quasi-static reference allowing calculating the DIF (Eq. 5) and the slip profile allows calculating the slip rate as the gradient of the slip-time curve. Similar procedures were used previously (Hao and Tarasov [17], Pereira et al [18], Lourenço and Pereira [19]).

$$DIF = \frac{Property\ (dynamic)}{Property\ (quasi-static)}, f(\dot{\delta}) \quad (5)$$

Different test setups have been used to characterize the bond behaviour of concrete-FRP systems, some being already implemented in international standards such as the American Concrete Institute (ACI 440). In the case of masonry-FRP systems, due to the lack of standard test setups, similar setups have been used to study this phenomenon (Ghiassi [24]). Single-lap shear bond tests consist in imposing a load in the FRP strip, along its longitudinal direction (Figure 3a). Usually, the composite is applied to one of the faces of the substrate, leaving enough FRP strip free to be connected to the actuators.

Ghiassi [24] studied the bond behaviour of GFRP-brick systems using single-lap shear bond tests under quasi-static conditions. These tests were performed with similar specimens to those studied in this work, using the same materials. These tests under quasi-static regime were performed using a servo-hydraulic actuator with a 50 kN maximum capacity. The test specimens were placed in a steel support structure (Figure 3b), specially designed for this purpose. The load profile was measured using a load cell and the slip was measured using several LVDTs placed along the reinforcement (Figure 3c). Five tests were performed (Figure 4) averaging a maximum load of 9.22 kN (Figure 4a) and a maximum slip of 1.43 mm (Figure 4b). These tests were performed under a slip rate of around 10^{-5} mm/ms. These results are used in this work as the quasi-static reference for the DIF calculation.

In order to study the bond behaviour of these systems under high strain rates, a new test setup was developed based on the drop weight concept. This new testing equipment and the obtained results are presented in the following sections.

4.1. Testing equipment

A drop weight tower specifically developed for single-lap shear bond tests was used for the dynamic testing (Figure 5a). This tower allows a drop height up to 3 meters and a drop weight with a minimum of 14 kg.

The load profile was measured at the free end of the GFRP strip using a load cell specifically for dynamic applications – VETEK VZ101BH (Figure 5b). This load cell is connected to a National Instruments Acquisition System. This acquisition system is composed of a SCXI-1000DC chassis (Figure 5c), a SCXI-1600 data acquisition and control card for PC connection and a generic input module SCXI-1520 with a SCXI-1314 mount. The SCXI-1600 limits the sampling speed to 200 kS/s (200 samples per millisecond), which was found to be enough even at a later stage where 4 channels where used at the same time, allowing an acquisition frequency of 50 kHz per channel.

The deformation behaviour of the specimen was measured in two different ways. First, a FastCam video camera was used. It is a PHOTRON FastCam APX – RS (Figure 5d) with a maximum frame rate of 250 000 frames per second. This equipment allowed the visualization of the test in slow motion and the measuring of the slip. This slip measurement was possible using targets in the specimen at a specific location and performing a tracking sweep of those targets in the video (Figure 6a). To perform the tracking sweep, the TEMA Tracking Software (v: 3.1-005) was used. With the relative position of the targets, the slip at each instance was calculated. The second methodology used to obtain the deformation behaviour was using strain gauges. The strain gauges used were BFLA-5-8-3L (Figure 6b) from TML and were the same used in the quasi-static testing performed by Ghiassi [24].

4.2. Specimens preparation

The application of GFRP reinforcement usually involves two steps: a) preparation of the substrate surface and b) application of the reinforcement. The preparation of the substrate surface, in this case clay brick, should be taken with special attention in order to obtain a good bond between the two materials (Juvantes [25]). The bricks used in this study, 200x100x55 mm bricks, were similar to those already studied and characterized previously by Pereira et al [18], Lourenço and Pereira [19] and Ghiassi [24] under different conditions. Initially the bricks were grinded (approximately 7 mm) in the face where the reinforcement was applied, in order to improve the mechanical and chemical bond capacity of the application (Ghiassi [24]). After this initial treatment the bricks were washed and placed in an oven at 100 ºC for a period of 24 hours. After this period the specimens were removed from the oven and cleaned with compressed air, making sure that the surface was kept clear of any small particles.

With the surface prepared, the reinforcement application can be initiated. Firstly, a primer is applied, only in the bonded area (the rest of the surface is protected with duct-tape) (Figure 7a). The applied primer was a MAPEWARP PRIMER 1 and the bonded area can be seen in Figure 7b. The GFRP reinforcement was composed of glass fibre MAPEWRAP UNI-AX and MAPEWRAP 31 epoxy. In order to apply the reinforcement, the procedure was the following:

a) Cut the glass fibres with the required dimensions (400x50 mm) and place two metallic sheets in one end of the fibres for bracing (Figure 7b);
b) In the brick surface a layer of epoxy is applied using a brush;
c) In the fibres a layer of epoxy is also applied and the fibres are placed in the correct position. In order to have full contact between the fibres and the surface a foam roll is used;

d) A new layer of epoxy is applied on top of the fibres and the foam roll is also used to have an even distribution of the epoxy;
e) After 60 minutes the duct tape is removed and the specimens are left to cure at ambient conditions for three weeks (Figure 7c).

It should be noted that the bond behaviour of these strengthening systems is much dependant on the preparation of the specimens. Although the specimens used for impact testing were not from the same batch as the specimens used for the quasi-static tests from Ghiassi [24], the same procedure was used and the same technician supervised the preparation of both batches.

4.3. Impact test results

A total of 20 specimens were tested with the drop-weight tower developed for dynamic testing. Five tests were not considered in this document due to failure of acquiring data during the test. The hammer weight was kept at 14 kg and the drop height varied from 10 to 40 cm. By varying the drop height, different impact energies are introduced in the system leading to different strain rates. The acquisition sampling speed was kept at 24 kHz for the force and strain profiles and 12000 fps for the video equipment. Figure 8 shows two examples for low (I37 – 0.2 mm/ms) and high (I30 – 1.0 mm/ms) slip rates of force profile (Figure 8a), slip profiles (Figure 8b) and force-slip profiles (Figure 8c). Figure 9 shows the typical failure modes obtained in the dynamic single-lap shear bond tests, being similar to those obtained in the quasi-static tests by Ghiassi [24].

Table 1 shows the results obtained for the dynamic tests on GFRP-brick systems. It can be seen that the maximum force ranged from 12.65 kN to 18.73 kN for slip rates of 0.06 mm/ms and 1.32 mm/ms, respectively. The slip rate was calculated as the gradient of

the slip-time curve, similar procedure for strain rates was previously used (Hao and Tarasov [17], Pereira et al [18])

It is clear that the slip rate influences the bond behaviour of these systems. For slip rates of around 1 mm/ms the maximum force is about two times the maximum force obtained for the same system under quasi-static conditions. This is equivalent to a 14 kg mass being dropped at 40 cm. Using the quasi-static reference values from Ghiassi [24] it is possible to calculate a Dynamic Increase Factor, as the relation between both the reference and the dynamic test. With the relation between the Dynamic Increase Factor (DIF) for the maximum force and the slip rate, it is clear how the slip rate influences the bond behaviour of these systems (Figure 10). A trendline was obtained for slip rates between 0.06 and 1.32 mm/ms (range of the performed tests). It was assumed that the trendline would start, with the same orientation, from a DIF value of 1.00. Is was also assumed that from the quasi-static slip rate until the point where the regime changes to dynamic, the DIF remains constant and equal to 1.00. Further testing for smaller slip rates is required to validate these assumptions.

The empirical relation that is able to translate the influence of the slip rate in the maximum force of these GFRP-brick, based on the obtained trendline, can be presented as Eq. (6), being the slip rate in mm/ms. This log-linear relation has an R^2 of 75%, which can be considered reasonable taking into consideration the nature of these materials and these tests.

$$DIF(F_{MAX}) = \begin{cases} 1 & if \quad 2E-5 < \dot{\delta} < 2.71E-3 \\ 0{,}1554 \ln(\dot{\varepsilon}) + 1.9184 & if \quad 2.71E-3 < \dot{\delta} < 1.32 \end{cases} \tag{6}$$

As stated previously, tests using strain gauges were also performed. The two main reasons for using the strain gauges are: (a) validate the video equipment acquisition system, by comparing the slip from the two different sources; (b) determine the

effective bond length in this dynamic regime. Three strain gauges were placed in each specimen (50 mm spaced), as can be seen in Figure 7b. Figure 11 shows two examples of the results obtained with strain gauges, for total detachment of the fabric (Figure 11a) and partial detachment of the fabric (Figure 11b). As can be been in Figure 11 when the first strain gauge is in plateau at maximum strain, the next strain gauge is registering a very low strain value, close to zero. Knowing that the strain gauges are spaced 50 mm, the effective bond length was considered to be 50 mm or less. This result for the effective bond length is similar to the results obtained for the quasi-static regime, where the same value for the effective bond length was determined by Ghiassi [24] meaning that the slip rate does not influence the effective bond length of these systems. Because when there is a detachment longer than the effective bond length, the maximum force is already mobilized, this allow the inclusion of the experimental tests with a partial detachment of 50 mm or higher in this analysis (Table 1; Figure 11).

As presented by Oliveira et al [26] and previously used by Ghiassi [24] it is possible to estimate the slip profile (Figure 12) knowing the strain distribution along the reinforcement at different instances, using the following:

$$\delta = \int \varepsilon(x)\, dx \tag{7}$$

With the slip profile obtained from the tests with strain gauges (Figure 12), it is possible to compare these results with the ones obtained with the video tracking acquisition. Table 2 shows the results obtained for the two different acquisition systems for the selected specimens. Regarding the maximum slip, the results are very similar with the exception of specimen I30 where the video equipment suggests almost the double of the maximum slip suggested by the strain gauges. Regarding the slip rate, the results are similar between both acquisitions. Adding these new results, obtained with strain

gauges, to the results obtained with the video tracking acquisition (Figure 13) it is possible to see that these values fit perfectly in the range obtained with the video equipment, giving confidence in the obtained results. It is important to notice that considering only the results from the strain gauges, the obtained trendline would have a R^2 of 95%. Although the smaller sample size (4 values) does have an impact in this value, it seems that using strain gauges would improve the overall quality of the results. However this technique increases considerably the costs involved in these experimental studies.

5. Conclusions

An experimental campaign was performed to study the bond behaviour of GFRP systems applied on clay bricks. Single-lap shear bond tests were considered to be the most representative to study the bond behaviour of these systems under impulsive loading. A new drop weight tower was developed specifically for this purpose allowing masses over 14 kg and drop heights up to 3 meters. By varying the drop height it was possible to introduce in the systems different slip rates, ranging from 0.06 mm/ms to 1.32 mm/ms.

From the obtained results it is clear that the slip rate influences the bond behaviour of these systems. These results show that for slip rates of around 1 mm/ms there is an increase of the maximum bond capacity of about two times the quasi-static value (with slip rate of 10^{-5} mm/ms). These results, obtained with video tracking, were validated with strain gauges along the reinforcement in some of the tests. These tests with strain gauges also allowed determining the effective bond length, being the same as the obtained in quasi-static regime. Leading to conclude that the slip rate does not influence

the effective bond length of these systems, similar to what has been observed by Al-Zubaidy [9].

The log-linear empirical relation translating the influence of the slip rate on the DIF for the bond capacity of CFRP-Brick systems has been presented up to 1.32 mm/ms. This empirical relation was assumed to be constant and equal to one from the quasi-static slip rate until the intersection point with the trendline of the impulsive regime (2.7E-3 mm/ms). Additional tests with slip rates between 2.7E-3 mm/ms and 0.1 mm/ms are required to validate this assumption. Also additional tests with slip rates higher than 1 mm/ms are required in order to verify if the proposed relation is valid for higher slip rates or if the slope of the trendline changes. It should be noted that these results show the bond behaviour between brick and GFRP and caution should be taken when considering masonry structures (brick and mortar). The same type of experiments on masonry units should be performed in order to evaluate possible differences in the bond behaviour under high strain rates.

The failure modes obtained with these experimental tests under impulsive loading were characterized by the ripping of a thin layer of brick. These failure modes are similar to those obtained for quasi-static regime, leading to assume that the slip rate does not influences the failure mode of these systems, similar to the observed by Al-Zubaidy [9].

As shown in this work the slip rate or the strain rate (depending on what is measured) has considerable influence in the response of materials, including the bond behaviour of modern reinforcement techniques and materials such as GFRP. This influence has to be considered in the modelling and design of these systems under impulsive loading such as impacts or blast loading, and need to be incorporated in the constitutive models of

these materials under non-linear analysis; similar to what has been done previously for masonry by Lourenço et al [27].

6. Acknowledgement

This work was performed under Project CH-SECURE (PTDC/EMC/120118/2010) funded by the Portuguese Foundation of Science and Technology – FCT. The authors acknowledge the support. The first author also acknowledges the support from his PhD FCT grant with the reference SFRH/BD/45436/2008.

7. References

[1] Meyers MA. *Dynamic behaviour of materials*. John Wiley & Sons Publications, USA 1994.

[2] Hiermaier SJ. *Structures under crash and impact – continuum mechanics, discretization and experimental characterization*. Springer Publications, Germany 2008.

[3] Ngo T, Mendis P, Hongwei M, Mak S. *High strain rate behaviour of concrete cylinders subjected to uniaxial compressive impact loading*. In Proc. of the 18th Australasian Conference on the Mechanics of Structures and Materials, Australia, 2004.

[4] Stavrogin AN, Tarasov BG. *Experimental physics and rock mechanics*. Balkema Publications, India 2001.

[5] Baylot J, Bullock B, Slawson T, Woodson S. *Blast response of lightly attached concrete masonry unit walls*. Journal of Structural Engineering 2005; 131(8): 1186-1193.

[6] Moreland C, Hao H, Wu CQ. *Response of retrofitted masonry walls to blast loading*. In Proc. of the 6th Asia-Pacific Conference on Shock and Impact Loads on Structures, Australia 2005.

[7] Bakis CE, Bank LC, Brown VL, Cosenza E, Davalos JF, Lesko JJ, Mashida A, Rizkalla SH, Triantafillou TC. *Fiber-Reinforced Polymer Composites for*

Construction – State-of-the-art Review. Journal of Composites for Construction 2002; 6(2):73-87.

[8] Panpazopoulou SJ, Tastani SP, Thermou GE, Triantafillou T, Monti G, Bournas D, Guadagnini M. *Background to European seismic design provisions for the retrofit of RC elements using FRP materials.* Structural Concrete 2015; DOI: 10.1002/suco.201500102.

[9] Al-Zubaidy H, Xiao-Ling Z, Al-Mihaidi R. *Experimental investigation of bond characteristics between CFRP fabrics and steel plate joints under impact tensile loads*. Composite Structures 2012; 94(2):510-518.

[10] Shi J, Zhu H, Wu Z, Wu G. *Experimental study of the strain rate effect of FRP sheet-concrete interface*. Tumu Gongcheng Xuebao/ China Civil Engineering Journal 2012; 45(12):99-107.

[11] Li XQ, Yang ZJ, Chen JF, Lu Y. *Loading rate effect on FRP-to-concrete Bond Behaviour*. Advanced Materials Research 2011; 250: 3571-3576.

[12] Shen D, Shi X, Ji Y, Yin F. *Strain rate effect on bond stress-slip relationship between basalt fiber-reinforced polymer sheet and concrete.* Journal of Reinferced Plastics & Composites 2015; 34(7):547-563.

[13] Grote D, Park S, Zhou M. *Dynamic behaviour of concrete at high strain rates and pressures.* Journal of Impact Engineering 2001; 25(9): 869-886.

[14] Malvar LJ, Ross CA. *Review of static and dynamic properties of steel reinforcement bars.* ACI Material Journal 1998; 95(5): 609-616.

[15] CEB-FIP. *Comité euro-international du betón – model code 2010 – final draft*. Thomas Thelford Publications, Switzerland 2010.

[16] UFC 3-340-02. *Structures to resist the effects of accidental explosions.* Department of Defence, USA 2008.

[17] Hao H, Tarasov BG. *Experimental study of dynamic material properties of clay brick and mortar at different strain rates.* Australian Journal of Structural Engineering 2008; 8(2):117-132.

[18] Pereira JM, Dias A, Lourenço PB. *Dynamic properties of clay brick at different strain rates.* 12th Canadian Masonry Symposium, Vancouver 2013.

[19] Lourenço PB, Pereira JM. *Characterization of masonry behaviour under high strain rates.* SAHC2014 – 9th International Conference on Structural Analysis of Historical Constructions, Mexico 2014.

[20] Asprone D, Cadoni E, Prota A, Manfredi G. *Dynamic behaviour of a Mediterranean natural stone under tensile loading*. International Journal of Rock Mechanics and Mining Sciences 2009; 46(3):514-520.

[21] Gurusideswar S, Velmurugan R. *High strain rate sensitivity of glass/epoxy/clay nanocomposites*. ICCST/10 – International Conference on Composite Science and Technology, Lisbon 2015.

[22] Okoli O. *The effects of strain rate and failure modes on the failure energy of fiber reinforced composites*. Composite Structures 2001; 54:299-303.

[23] Correia P, Peixinho N. *Static and Dynamic Tensile Behavior of Unidirectional Glass/Epoxy Composites*. Advanced Materials Research 2014; 1016:298-301.

[24] Ghiassi B. *Durability analysis of bond between composite materials and masonry substrates*. PhD-thesis, University of Minho, Portugal 2013.

[25] Juvantes LFP. *Strengthening and reinforcement of reinforced concrete structures using CFRP composites*. PhD-thesis, University of Porto, Portugal, 1999.

[26] Oliveira DV, Basilio I, Lourenço PB. *Experimental bond behaviour of FRP sheets glued on brick masonry*. Journal of Composite for Construction 2010; 14(3):312-323.

[27] Lourenço PB, Rafsanjani SH, Pereira JM. *A constitutive three-dimensional interface model for masonry walls subjected to high strain rates*. The twelfth International Conference on Computational Structures Technology, Italy 2014.

Table captions:

Table 1 – Impact tests on GFRP-brick specimens.

Table 2 – Comparison between video equipment and strain gauges results.

Figure captions:

Figure 1 – DIFs for clay brick mechanical properties (Pereira et al [18], Lourenço and Pereira [19]).

Figure 2 – GFRP strips tensile strength at different strain rates by Correia and Peixinho[23].

Figure 3 – Single-lap shear bond tests: a) test schematic; b) steel support structure; c) LVDT positioning (Ghiassi [24]).

Figure 4 – GFRP-brick quasi-static results: a) force-time profile; b) slip-time profile (Ghiassi [24]).

Figure 5 – Test setup: a) drop weight tower setup; b) load cell; c) acquisition system; d) video equipment.
(1) Photron video equipment; (2) Drop weight tower; (3) load cell; (4) hammer; (5) specimen; (6) acquisition systems; (7) PC; (8) Strain gauges.

Figure 6 – Deformation acquisition: a) targets for video tracking; b) strain gauges.

Figure 7 – Specimens: a) specimen preparation; b) specimen geometry; c) final aspect of the specimens.

Figure 8 – Examples of impact test results: a) force-time profile; b) slip-time profile; c) force-slip profile.

Figure 9 – Examples of failure modes: a) total detachment of the fabric; b) partial detachment of the fabric.

Figure 10 – Dynamic increase factor for shear capacity at different slip rates.

Figure 11 – Examples of strain gauges signal acquisition: a) total detachment of the fabric; b) partial detachment of the fabric.

Figure 12 – Example of slip-time profile obtained from strain gauges.

Figure 13 – Dynamic increase factor for shear capacity of GFRP-brick at different slip rates.

Table 1 – Impact tests on GFRP-brick specimens.

Specimen	Drop height (cm)	PHOTRON		Load cell	DIF	Failure mode (Detachment length)
		Maximum slip (mm)	Slip rate (mm/ms)	Maximum force (kN)		
Quasi-static [19]		1.49	2E-5	9.22	1.00	Total
I37	11	0.19	0.06	12.65	1.37	Partial 5cm
I41	15	0.32	0.07	14.97	1.62	Partial 5cm
I7	16	0.17	0.08	14.66	1.59	Partial 7cm
I25	14	0.14	0.09	13.16	1.43	Partial 5cm
I1	17	0.29	0.10	14.94	1.62	Partial 6cm
I20	16	0.45	0.13	14,85	1.61	Partial 6cm
I40	19	0.49	0.15	15.96	1.50	Partial 7cm
I26	21	0.41	0.25	16.81	1.82	Total
I3	18	0.53	0.44	17.66	1.92	Partial 5cm
I31	25	0.76	0.57	16.65	1.81	Total
I46	30	0.84	0.74	17.15	1.86	Total
I44	31	0.87	0.77	17.64	1.91	Total
I36	28	0.58	0.83	15.64	1.70	Total
I30	37	1.00	0.87	17.29	1.88	Total
I49	36	1.28	1.32	18.73	2.03	Total

Table 2 – Comparison between video equipment and strain gauges results.

	Strain Gauges			PHOTRON			
Specimen	**Max Slip (mm)**	**Slip rate (mm/ms)**	**Strain rate (/s)**	**Max Slip (mm)**	**Slip rate (mm/ms)**	**Force (kN)**	**DIF**
I41	0.31	0.10	2.6	0.32	0.07	14.97	1.62
I40	0.36	0.23	2.5	0.49	0.15	15.96	1.73
I46	0.86	0.70	3.7	0.84	0.74	17.15	1.86
I30	0.56	0.98	7.4	1.00	0.87	17.29	1.88

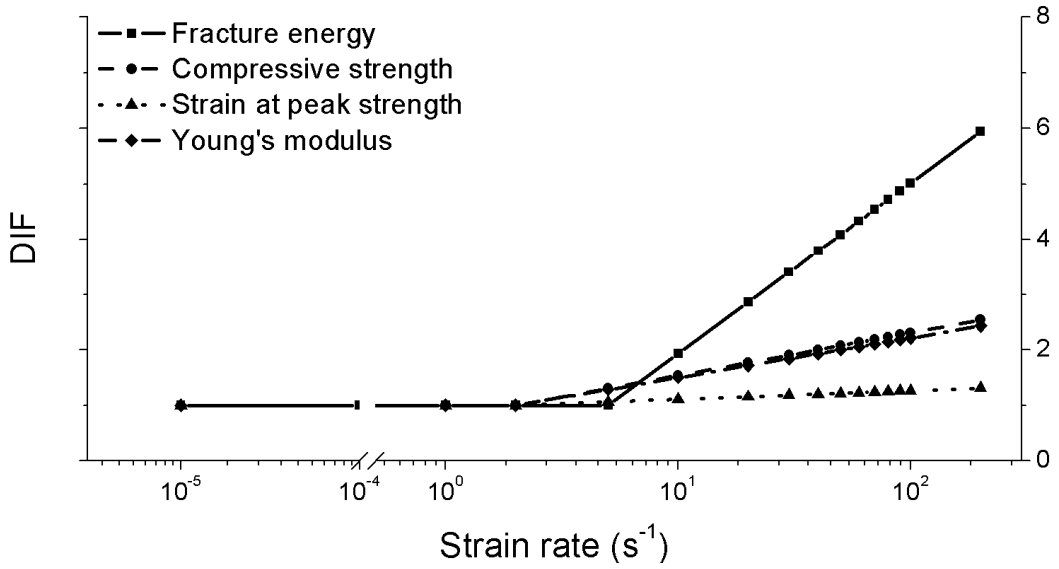

Figure 1 – DIFs for clay brick mechanical properties (Pereira et al [18], Lourenço and Pereira [19]).

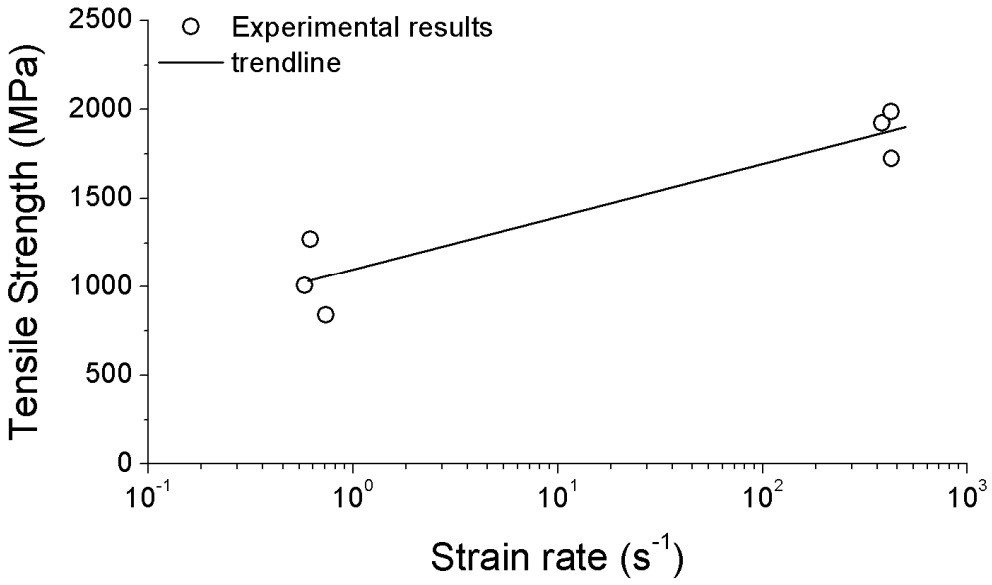

Figure 2 – GFRP strips tensile strength at different strain rates by Correia and Peixinho[23].

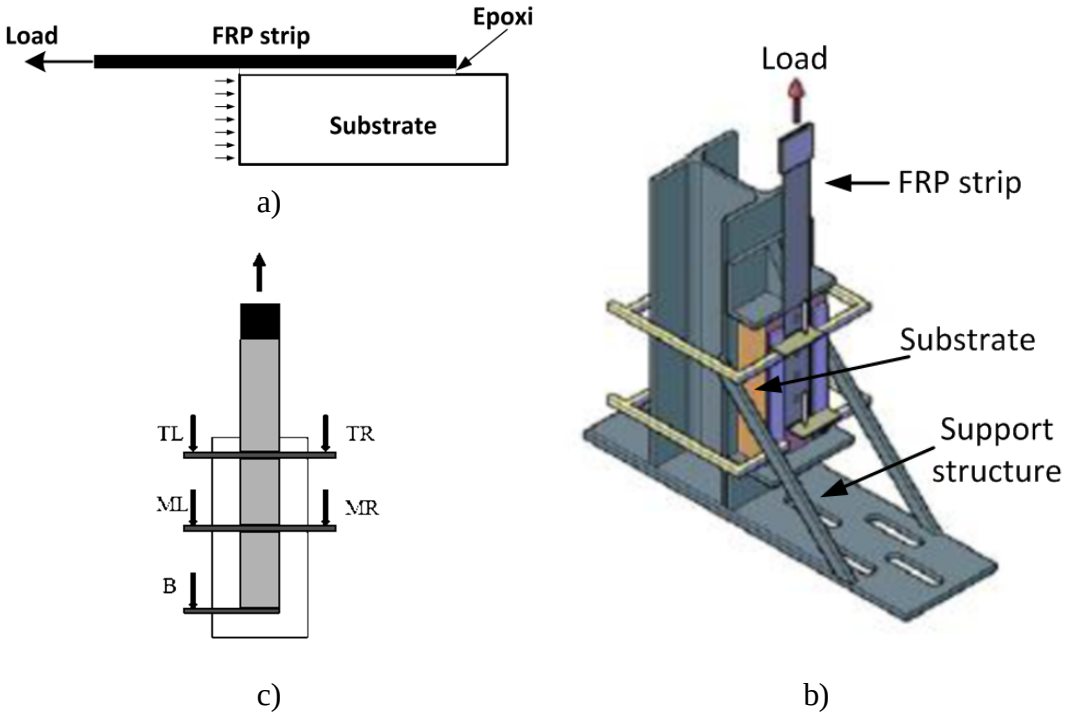

Figure 3 – Single-lap shear bond tests: a) test schematic; b) steel support structure; c) LVDT positioning (Ghiassi [24]).

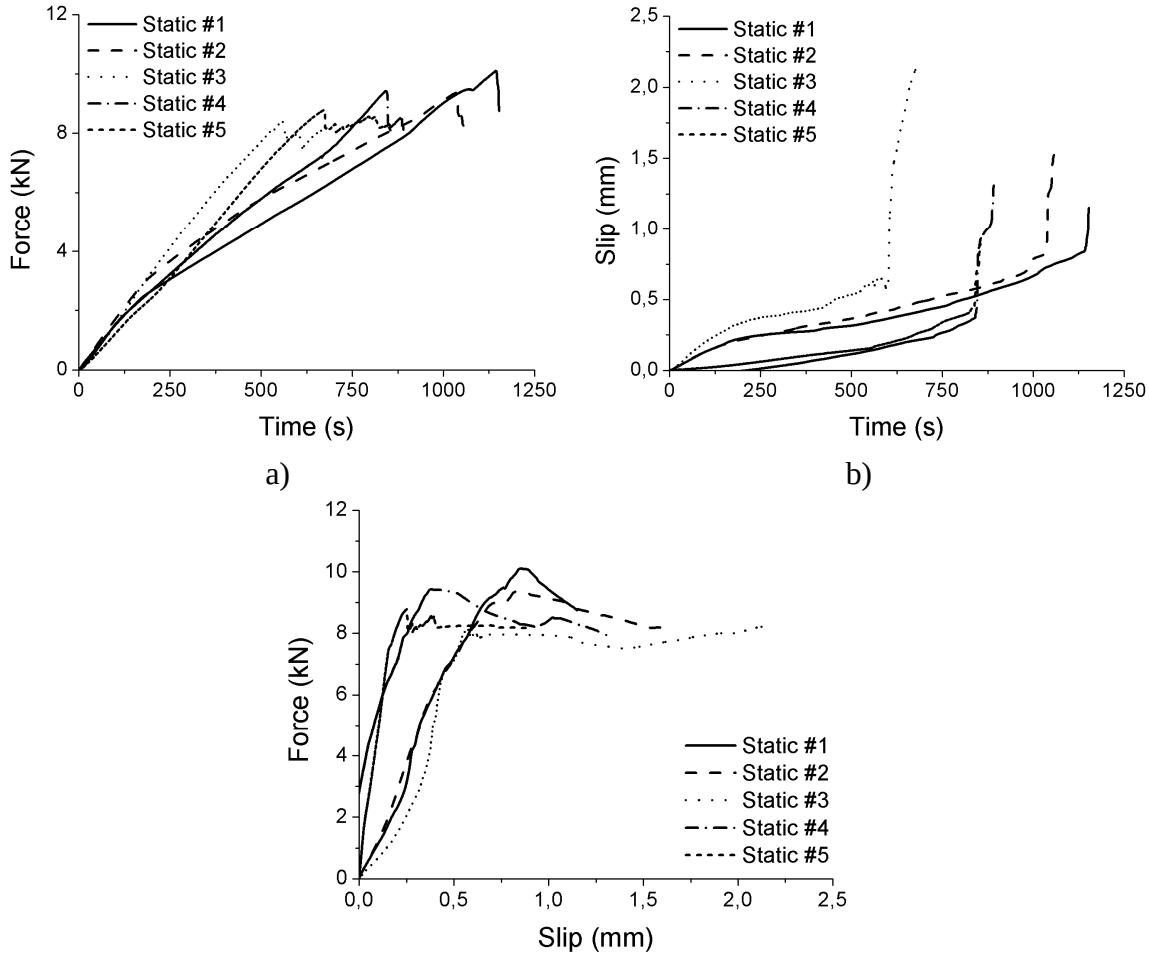

Figure 4 – GFRP-brick quasi-static results: a) force-time profile; b) slip-time profile (Ghiassi [24]).

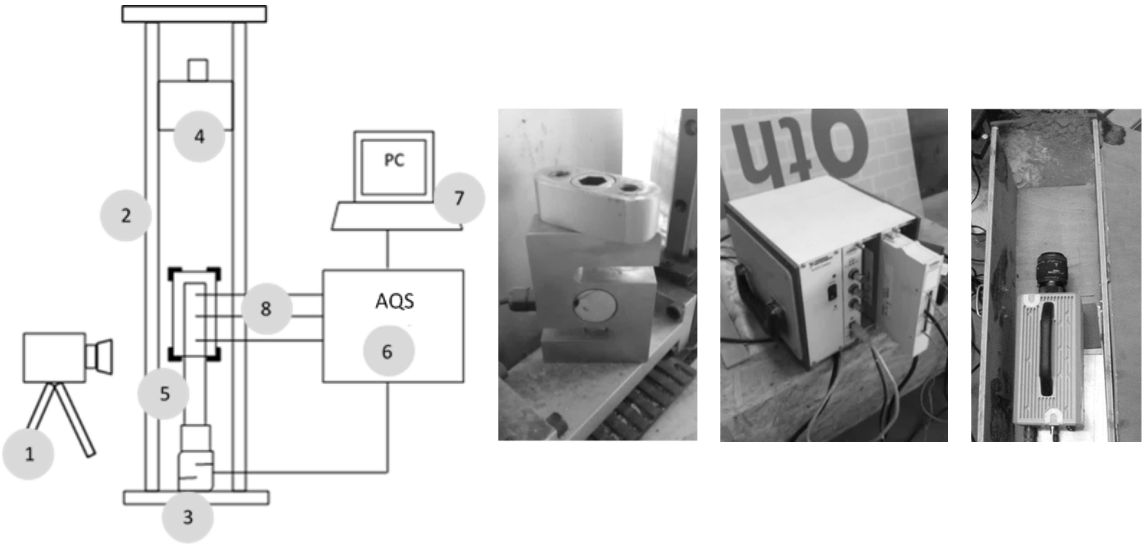

a) b) c) d)

Figure 5 – Test setup: a) drop weight tower setup; b) load cell; c) acquisition system; d) video equipment.

(1) Photron video equipment; (2) Drop weight tower; (3) load cell; (4) hammer; (5) specimen; (6) acquisition systems; (7) PC; (8) Strain gauges.

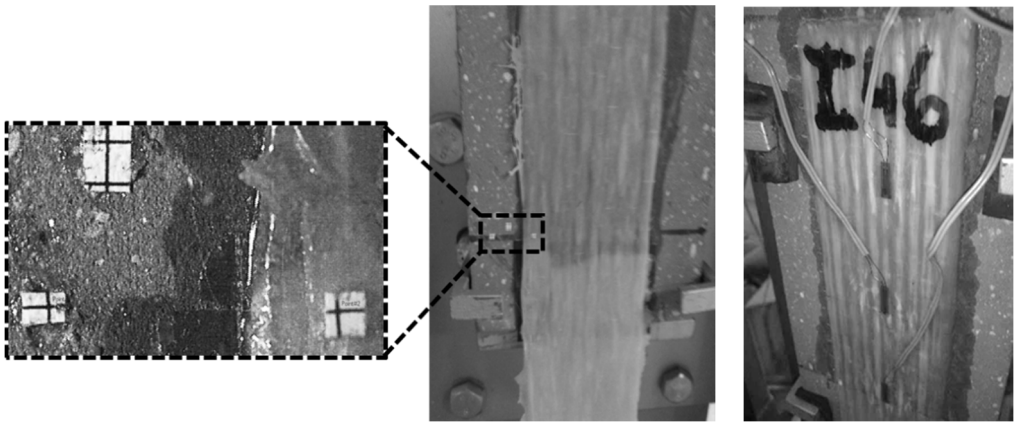

a) b)

Figure 6 – Deformation acquisition: a) targets for video tracking; b) strain gauges.

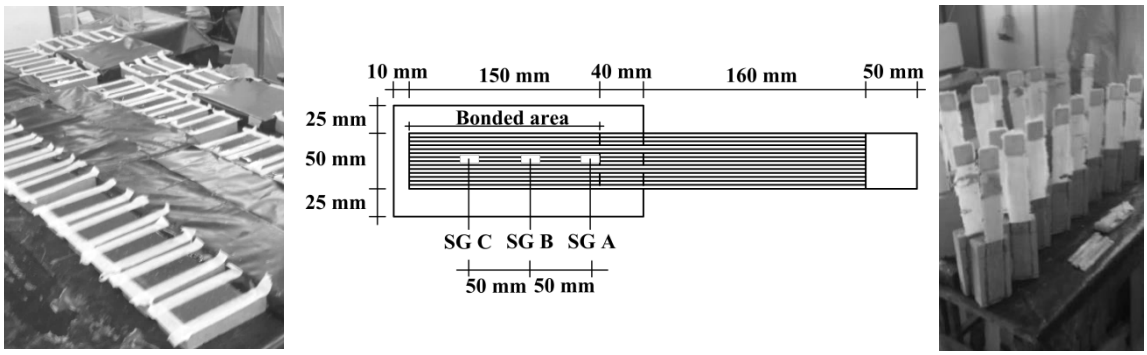

a) b) c)

Figure 7 – Specimens: a) specimen preparation; b) specimen geometry; c) final aspect of the specimens.

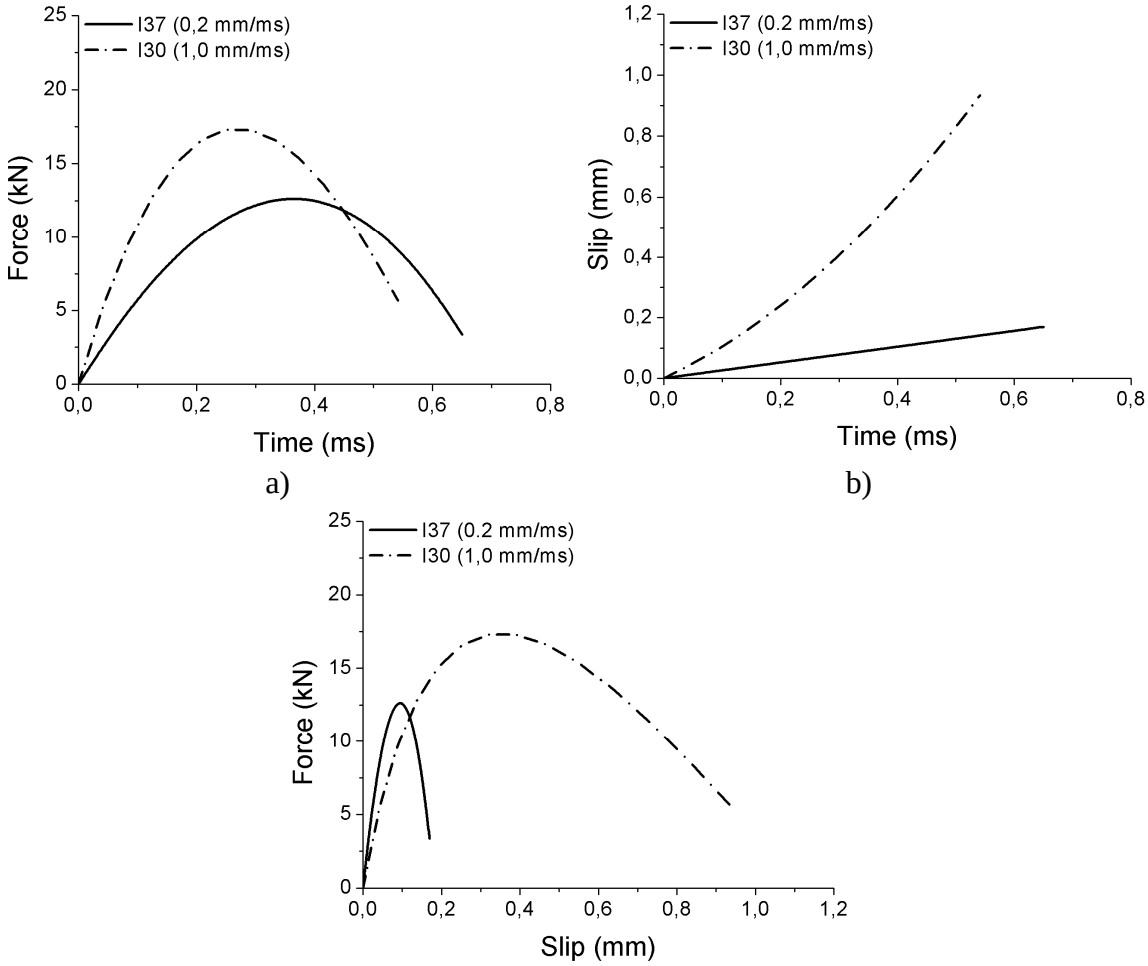

Figure 8 – Examples of impact test results: a) force-time profile; b) slip-time profile; c) force-slip profile.

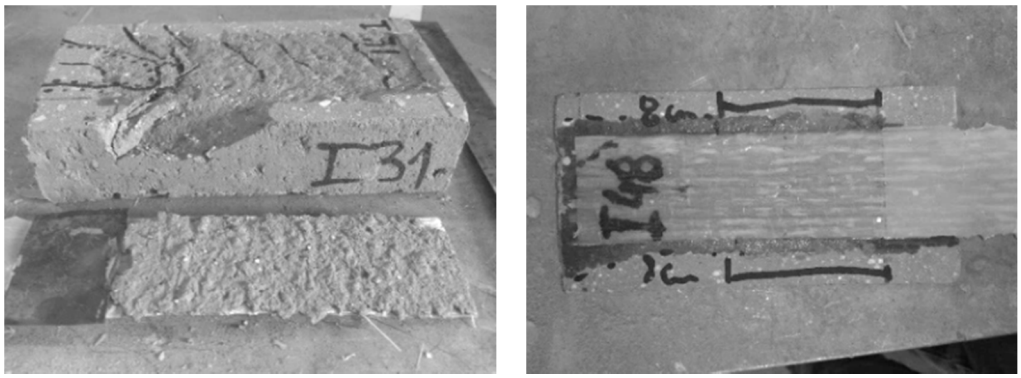

a) b)

Figure 9 – Examples of failure modes: a) total detachment of the fabric; b) partial detachment of the fabric.

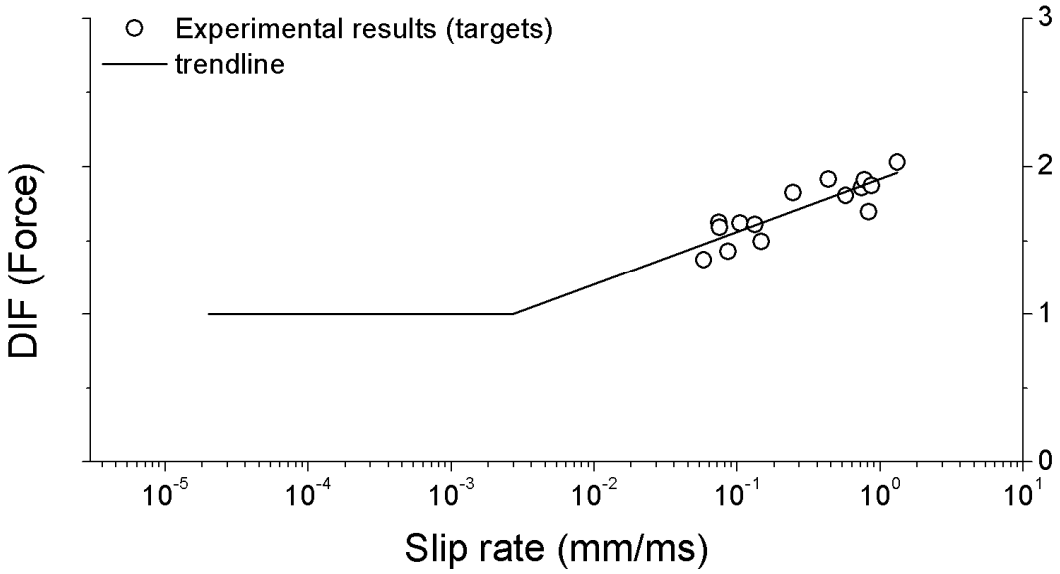

Figure 10 – Dynamic increase factor for shear capacity at different slip rates.

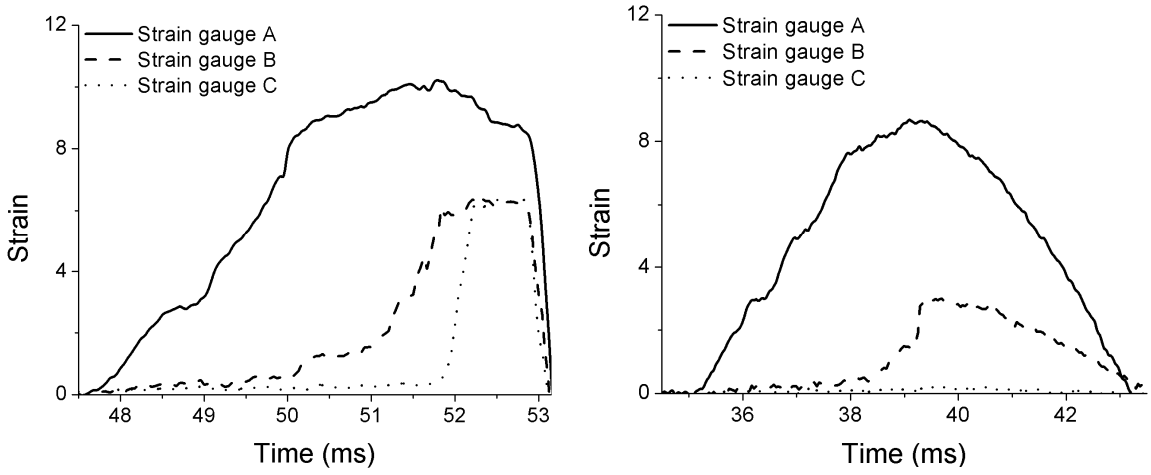

a) b)

Figure 11 – Examples of strain gauges signal acquisition: a) total detachment of the fabric; b) partial detachment of the fabric.

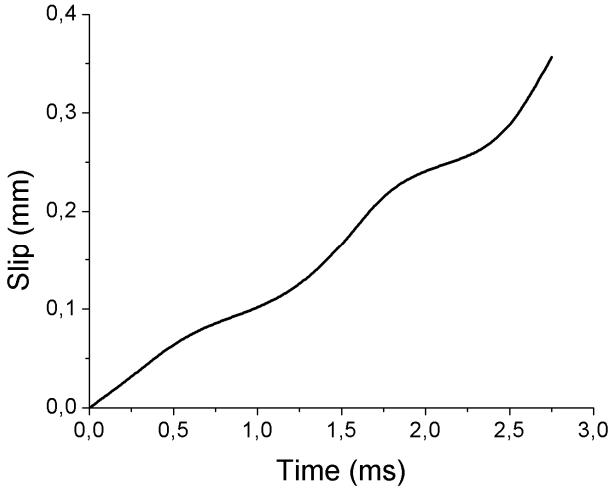

Figure 12 – Example of slip-time profile obtained from strain gauges.

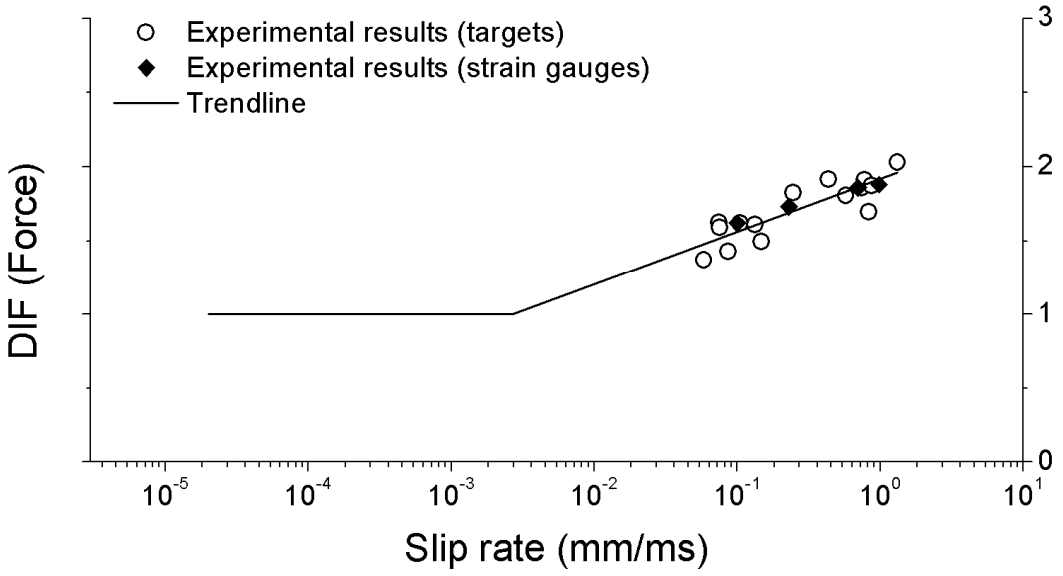

Figure 13 – Dynamic increase factor for shear capacity of GFRP-brick at different slip rates.